Posted on 22 Nov 2022 — The copyright holder is the author/funder. All rights reserved. No reuse without permission. — https://doi.org/10.1002/essoar.10508552.1 — This a preprint and has not been peer reviewed. Data may be preliminary.

Reconstructions and predictions of the global carbon cycle with an emission-driven Earth System Model

Hongmei Li[1], Tatiana Ilyina[2], Tammas Francis Loughran[3], and Julia Pongratz[4]

[1]Max Planck Institute for Meteorology
[2]Max Planck Institute of Meteorology
[3]Ludwig Maximilian University
[4]Ludwig-Maximilians Universität

November 22, 2022

Abstract

The global carbon budget including fluxes of CO2 between atmosphere, land and ocean, and its atmospheric growth rate show large interannual to decadal variations. Yet, these variations are poorly represented in uninitialized simulations. In a novel approach we reconstruct and predict the global carbon cycle with the decadal prediction system based on the Max Planck Institute Earth system model (MPI-ESM) extended with an interactive carbon cycle. By assimilating atmospheric and oceanic data products into the MPI-ESM, we can well reproduce historical global carbon budget variations with high correlations relative to the assessments from the global carbon project of 0.75, 0.75 and 0.97 for atmospheric CO2 growth, air-land CO2 fluxes and air-sea CO2 fluxes, respectively. Retrospective predictions initializing from the assimilation simulation show the predictive skill of the air-sea CO2 fluxes up to 5 years, and the air-land CO2 fluxes and atmospheric carbon growth rate of 2 years.

Reconstructions and predictions of the global carbon cycle with an emission-driven Earth System Model

H. Li[1], T. Ilyina[1], T. Loughran[2], J. Pongratz[1,2]

[1]Max Planck Institute for Meteorology, Hamburg, Germany
[2]Department of Geography, Ludwig-Maximilians-Universität, Munich, Germany

Key Points:

- The global carbon cycle is well reproduced by MPI-ESM assimilation, which enables global carbon budgeting within a closed Earth system.
- Predictive skill of air-sea CO_2 fluxes is up to 5 years and it is up to 2 years for air-land CO_2 fluxes and the atmospheric carbon growth.
- For the first time, our emission-driven predictions enables prognostic atmospheric CO_2, hence reconstructing and predicting the variations.

Corresponding author: Hongmei Li, hongmei.li@mpimet.mpg.de

Abstract

The global carbon budget including fluxes of CO_2 between atmosphere, land and ocean, and its atmospheric growth rate show large interannual to decadal variations. Yet, these variations are poorly represented in uninitialized simulations. In a novel approach we reconstruct and predict the global carbon cycle with the decadal prediction system based on the Max Planck Institute Earth system model (MPI-ESM) extended with an interactive carbon cycle. By assimilating atmospheric and oceanic data products into the MPI-ESM, we can well reproduce historical global carbon budget variations with high correlations relative to the assessments from the global carbon project of 0.75, 0.75 and 0.97 for atmospheric CO_2 growth, air-land CO_2 fluxes and air-sea CO_2 fluxes, respectively. Retrospective predictions initializing from the assimilation simulation show the predictive skill of the air-sea CO_2 fluxes up to 5 years, and the air-land CO_2 fluxes and atmospheric carbon growth rate of 2 years.

Plain Language Summary

Reconstructing and predicting the variable global carbon cycle is essential for tracing the fate of carbon and the corresponding climate and ecosystem changes. Reconstructions based on the MPI-ESM emission-driven prediction system by assimilating observational products capture the observed global carbon budget variations in the past decades. Such a fully coupled decadal prediction system with interactive carbon cycle enables representation of the global carbon budget within a closed Earth system and therefore provides an additional line of evidence for the ongoing assessments of the anthropogenic global carbon budget. Retrospective predictions starting from the reconstruction show promising predictive skill for the global carbon cycle up to 5 years for the air-sea CO_2 fluxes and up to 2 years for the air-land CO_2 fluxes and atmospheric carbon growth rate. Our results also suggest predictions based on Earth system models enable reproduction and prediction of the evolution of atmospheric CO_2 concentration changes. The earth system predictions in this study provide valuable inputs for understanding the global carbon cycle and supporting climate relevant policy development.

1 Introduction

The CO_2 fluxes between atmosphere, land and ocean and thus the atmospheric carbon growth rate vary substantially on interannual to decadal time-scales (Peters et al., 2017; Friedlingstein et al., 2019; Landschützer et al., 2019; Friedlingstein et al., 2020). These variations reflect combined effects of internal variability of the global carbon cycle (Li & Ilyina, 2018; Séférian et al., 2018; Spring et al., 2020; Fransner et al., 2020) and its responses to external forcings (McKinley et al., 2020).

To constrain the global carbon cycle of the past and facilitate its prediction and projection into the future, since 2007 the Global Carbon Project (Canadell et al., 2007) assesses the anthropogenic global carbon budget (GCB), i.e., CO_2 emissions and their redistribution among the atmosphere, ocean, and land every year. This assessment is based on data assessments for emissions, observations of the atmospheric CO_2 concentration and single stand-alone model simulations, separately for ocean and land, of CO_2 fluxes. The air-land fluxes are the sum of natural fluxes and the land-use change induced emissions, the GCBs use the bookkeeping approach for the land-use emissions term. The stand-alone simulations on land and ocean use different climatology and thus do not provide an internally consistent estimate of the CO_2 fluxes. Moreover, these stand-alone model simulations of CO_2 fluxes do not exactly match the observations while the variations are well represented via constraining by observation/reanalysis data forcing. Therefore, the global carbon budget is not closed but ends up with a budget imbalance term up to 2 PgC/year (Friedlingstein et al., 2020), which hinders full attribution of the global carbon cycle variations. The budget imbalance could be also attributed to a large part to the mismatch of net biome production between the dynamic global vegetation models (DGVMs) used in the GCBs and inversions that match the atmospheric CO_2 growth rate (Bastos et al., 2020). Both DGVM spread and differences between inversions contributed substantially to the uncertainty of the budget terms on the global and regional scale, respectively (Bastos et al., 2020).

Reconstruction of the variable global carbon cycle within a closed Earth system model (ESM) is of essential value of tracing the fate of carbon and the corresponding climate and ecosystem changes. The decadal prediction systems based on ESMs (Marotzke et al., 2016) show potential to reconstruct and predict the global carbon cycle (Li et al., 2016; Spring & Ilyina, 2020). By assimilating observational products of physical fields, the decadal prediction systems show ability to reproduce the variations of CO_2 fluxes as found in observation-based products. Starting from initial states from the assimilation simulation that are close to the real world, decadal prediction systems enable further multi-year predictions of the global carbon cycle (Li et al., 2016, 2019; Lovenduski, Yeager, et al., 2019; Lovenduski, Bonan, et al., 2019; Ilyina et al., 2021). However, as of now, the state-of-the-art decadal prediction systems are typically forced with prescribed atmospheric CO_2 concentration without interactive carbon cycle, i.e., the feedback of CO_2 fluxes strength to the atmospheric CO_2 variations is ignored. With this conventional model setup, one can only assess the CO_2 fluxes into land and ocean, but not the resulting variations in atmospheric CO_2 concentration and growth.

For the first time, we extend our prediction system from concentration-driven to emission-driven taking into account the interactive carbon cycle and hence enabling prognostic atmospheric carbon increment. In this study, we assess the global carbon budget in a simulation with assimilating data products into the model, and further estimate our decadal predictions based on the Max Planck Institute Earth system model (MPI-ESM) relative to GCB2019 (Friedlingstein et al., 2019) and observation-based estimates of the CO_2 fluxes and atmospheric CO_2. The assimilation simulation is designed to reconstruct the evolution of climate and earth system of the real world by incorporating essential fields from observational products into the MPI-ESM. The reconstruction from the fully coupled model simulation (i.e., the assimilation simulation) enables representation of the global carbon budget within a closed Earth system. Therefore, by construction, this approach avoids the budget imbalance term arising from the need to budget carbon fluxes from stand-alone models and observations. Our reconstructions of the carbon budget provide an additional novel estimate, that could be used in addition for a consistent assessment of the dominant processes in regulating the global carbon cycle. The assimilation simulation states, which are close to the real world, are then used to start our retrospective prediction simulations (i.e., initialized simulations) aiming to predict the changes of global carbon cycle in the next years by improving the initial states.

2 Materials and Methods

2.1 Model and simulations

We use the MPI-ESM1.2-LR (Mauritsen et al., 2019), which is the low resolution version of MPI-ESM1.2 used for the sixth phase of the Coupled Model Intercomparison Project (CMIP6). The atmospheric horizontal resolution has a spectral truncation at T63 or approximately 200-km grid spacing with 47 vertical levels. The resolution of the ocean model MPIOM is about 150 km with 40 vertical levels. The ocean biogeochemistry component of MPI-ESM is represented by HAMOCC (Ilyina et al., 2013; Paulsen et al., 2017), and the land and vegetation component is represented by JSBACH (Reick et al., 2021).

Similar to our previous prediction system (Li et al., 2016, 2019), we performed 3 sets of simulations, i.e., (i) uninitialized freely historical simulations, (ii) assimilation simulation by nudging the observational signal of climate variations into the model, and (iii) initialized simulations (also refers to as hindcasts or retrospective predictions) starting from the assimilation simulation, to investigate the capacity of our model to reconstruct and predict the global carbon cycle. The assimilation run is needed for the initialized prediction simulations, and the uninitialized simulations are references to compare to and assess the improved predictability due to initialization. The major difference relative to the previous system (Li et al., 2016, 2019) is that this new prediction system is based on emission-driven simulations, which are forced by CO_2 emissions instead of prescribed atmospheric CO_2 concentration. In this way, the atmospheric CO_2 concentration is evolving in response to the interaction with the strength in CO_2 uptake/outgas of the land and ocean. The external forcing is CMIP6 historical extended to the SSP2-4.5 scenario. While the fossil fuel emissions are forced, the land-use change induced emissions are prognostic in the ESMs with LUH2 land use forcing. We use transient land use transitions and included natural disturbances with dynamic vegetation. An ensemble of 10 members is run for the uninitialized historical and initialized prediction simulations. The uninitialized ensembles are generated by starting from different year of the control simulation. The initialized ensembles are generated with lagged 1-day initialization. Note that the initialized 5-year long predictions start annually from November 1st for the period 1960-2018. More details of the simulations are summarized in Table S1.

2.2 Assimilation methods

Similar to our previous concentration-driven decadal prediction systems (Li et al., 2019), the assimilation is done with nudging the ocean 3-D temperature and salinity anomalies from the ECMWF ocean reanalysis system 4 (ORAS4) (Balmaseda et al., 2013) and the atmospheric 3-D full-field temperature, vorticity, divergence, and log surface pressure from ECMWF Re-Analysis ERA40 (Uppala et al., 2005) during the period 1960-1979 and ERA-Interim (Dee et al., 2011) during the period 1980-2018. The sea-ice concentration is nudged towards the National Snow and Ice Data Center (NSIDC) satellite observations (as described in (Bunzel et al., 2016)). The nudging is applied to every model time step but with different relaxation time, i.e., relative longer relaxation time of 10 days for the ocean temperature and salinity and shorter relaxation time of 6 hours, 24 hours and 48 hours for the atmospheric vorticity, temperature and pressure, and divergence, respectively. The chosen variables for assimilation and the respective relaxation time are according to previous investigations of decadal climate prediction based on MPI-ESM (Marotzke et al., 2016). Direct assimilation of the carbon cycle related variables is not included because of the limited available data; in the meanwhile, we found that the global carbon cycle is well represented from the assimilation of only physical variables (Li et al., 2016, 2019; Lovenduski, Yeager, et al., 2019; Lovenduski, Bonan, et al., 2019; Ilyina et al., 2021), and furthermore, our recent study based on a perfect model framework (i.e., based on preindustrial run of the model itself) revealed that direct assimilation of the global carbon cycle only bring trivial improvement of predictive skill of the global carbon cycle (Spring et al., 2021). To avoid spurious upwelling in the equatorial region caused by assimilation as investigated in (Park et al., 2018), we exclude the equatorial band of 5°S-5°N from data nudging of the ocean data.

2.3 Carbon budget decomposition with CBALONE simulations

The anthropogenic carbon budget is usually decomposed into 5 terms plus an imbalance: the two emissions terms from fossil-fuel and land-use changes, and the three sink terms natural terrestrial sink, ocean sink, and atmospheric growth. The fossil fuel emissions are prescribed as forcing, and terrestrial and ocean carbon sinks and atmospheric growth terms can be directly derived from the ESM. However, directly deducible from an ESM is only the net land-atmosphere exchange, which is the sum of land-use change emissions and the natural terrestrial sink. In order to separate the two land-related fluxes, we use a stand-alone component called CBALONE from JSBACH as a diagnostic for a direct comparison with the global carbon project (Friedlingstein et al., 2019). More details of the method on separating the land-use change induced emission can be found in Loughran et al. (2021). Two simulations, one with and one without land-use change, are conducted with the forcing of the assimilation run. The difference of the two simulations quantify the land-use change induced emission.

2.4 Predictive skill quantification

The initialized simulations are investigated according to their lead time, i.e., how many model years they have been integrated freely after restarting from the assimilation simulation (Boer et al., 2016). The time series of initialized simulations at lead time of 1 year (2-5 years) combine the 1st year (2-5 years) predictions from initialized simulations of all the starting years from 1959-2018. Bias correction is an unavoidable topic for decadal predictions due to initial shock, which varies with lead time, therefore, it was recommended to do bias correction when necessary according to the lead time (Boer et al., 2016). In this study, a bias correction is applied for the atmospheric CO_2 concentration as shown in Fig. 4.

The predictive skill is quantified mainly based on anomaly correlation coefficient, the anomalies are calculated by removing the respective climatology mean state. Here the climatology mean state is based on the ensemble mean of the focus time period, i.e., 1970-2018 for Fig. 1-3 and last 10 years for Fig. 4. For the atmospheric CO_2 concentration shown in Fig. 4, which has high correlations close to 1 with observations because of the coherent linear trends, we have also added root mean square error (RMSE) metric to investigate the added value of assimilation and initialization. The significance of the predictive skill is tested with a nonparametric bootstrap approach (Goddard et al., 2013).

3 Reconstruction of the global carbon budget

By incorporating observational signals, the assimilation simulation from decadal prediction system based on MPI-ESM captures the evolution of the global carbon cycle as well as the climate in observations. The time series from MPI-ESM assimilation simulation in comparison to the GCB2019 is shown in Fig.1.

The CO_2 emissions from fossil fuel and industry are in general consistent but with slightly difference in the 1960-1990s between the assimilation simulation (which uses the CO_2 emission forcing provided by CMIP6 for historical and SSP2-4.5 simulations) and GCB2019. This reveals uncertainty in the CO_2 forcings, which could affect the amplitude of the atmospheric CO_2 concentration as it is a cumulative quantity. Cumulatively the CMIP6 CO_2 emission forcing is 8.20 PgC higher than that from the GCB2019, which would end up with a 3.86 ppm (by dividing a factor of 2.124 PgC ppm-1 (Ballantyne et al., 2012)) higher atmospheric CO_2 concentration in the simulation with CMIP6 forcing than with GCB2019 forcing. This discrepancy of CO_2 emission might explain to some extent that the simulated atmospheric CO_2 concentration is few ppm higher than the NOAA_GML observation (Dlugokencky & Tans, 2020) (Fig. S1). However, this little difference of a few ppm in atmospheric CO_2 concentration magnitude doesn't noticeably affect the variations in the CO_2 fluxes and the corresponding atmospheric carbon increment (see Fig. 1D-F).

The land-use change induced emissions diagnosed by CBALONE are within the range of GCB2019 multi-model (including JSBACH) simulations from Dynamic Global Vegetation Models (DGVMs) (Fig.1B). The estimates from bookkeeping models show smaller variations as the DGVMs. Note that the GCBs use the bookkeeping approach for the land-use emissions term. Bookkeeping implies that carbon fluxes are determined from area changes in vegetation types of different vegetation and soil carbon densities, with specific response curves characterizing the evolution of decay and recovery. Carbon densities may stem from recent observations or models, but are kept fix, i.e. changes in environmental conditions are not accounted for. The DGVMs by contrast (which are used to provide only an uncertainty range around the bookkeeping models in the GCBs) calculate land-use emissions under transient environmental conditions. This implies first that interannual variability in bookkeeping models is only driven by land-use change, not further interactions with climate variability, which makes the DGVM estimates in general more variable from year to year than the bookkeeping estimates are. Second, it implies that the DGVM-based land-use emissions estimates include the so-called "loss of additional sink capacity" (Pongratz et al., 2014), which refers to the carbon that could have been stored on forests additionally over the course of history (e.g., due to the "CO_2-fertilization" effect) if these forests had not been cleared by expansion of agriculture and forestry. This loss of additionally sink capacity generally increases over time and amounts to about 40% (0.8±0.3 PgC yr^1) over 2009-2018 (Obermeier et al., 2021). This explains why DGVM estimates in Fig. 1B show higher emissions than bookkeeping estimates in recent decades. The DGVM- and expert-based uncertainty range around the GCB bookkeeping estimates is large and MPI-ESM-based land-use change emission estimates have been found to be at the high end of the GCB for all decades by Loughran et al. (2021), consistent with our findings.

There is a budget imbalance term resulting from the approach used in GCB2019 because the individual budget terms are from separate measurements together with standalone ocean and land model simulations (Friedlingstein et al., 2019). In this study, we assimilate each component within a fully coupled ESM considering the interactions. The assimilation ensures evolution of the carbon cycle and climate towards the real world, in the meanwhile, the budget is closed within the Earth system, i.e., no the budget imbalance occurs (Fig. 1C). Therefore, it is more reliable to attribute the global carbon budget variations using the assimilation simulation based on a fully coupled ESM.

Atmospheric carbon growth rate and carbon fluxes are reasonably well reproduced in emission-driven assimilation with prognostic atmospheric CO_2 (Fig. 1D-F). The atmospheric carbon growth and the land carbon sink show more pronounced variations on interannual time scales, however, the ocean carbon sink has more pronounced variations on decadal time scales. These variations are captured in the assimilation with high correlations between assimilation and GCB2019 of 075, 0.75, and 0.97 for atmospheric growth, land sink, and ocean sink, respectively.

The spatial distribution of coherence in carbon fluxes between GCB2019 and the MPI-ESM reconstruction is shown in Fig. S2. The correlation of CO_2 fluxes between reconstruction and GCB2019 is high, especially over the ocean. The root mean square deviation (RMSD) is coherent with the magnitude of carbon fluxes, i.e., with greater values on land than over ocean. The large RMSD is partially due to smoothed magnitude of fluxes in GCB2019 from multi-model mean.

In general, the historical global carbon cycle is well reproduced by the MPI-ESM with assimilating observational products, which enables quantification of the global carbon budget within a closed Earth system. Prediction systems can actually provide internally-consistent values of the ocean and land carbon sink and serve as an additional line of evidence for the global carbon budget. A full assimilation simulation spans a longer than the analysis period starting from year 1959 for which the reanalysis data is available, the first 12 years that might be affected by model adjustment were excluded from the analyses.

4 Predictability of global carbon cycle

The initialized predictions start from the assimilation states which are close to observations. Therefore, information of observation are incorporated into the prediction system as initial states and they facilitate that the evolution of the global carbon cycle and climate follow the trajectory of the real world for some period encompassing the predictability horizon.

As shown in Fig. 2, the initialized simulations at lead time of 2 years still resemble the variations well as in the GCB2019 with correlations of 0.49 and even higher. The results from lead time of 1 year is shown in Fig. S3. As for atmospheric carbon growth, the initialized simulations at lead time of 2 years show coherent interannual variations even with a relative smaller correlation (0.49) than that of the historical freely run (0.61), which is mainly contributed by the coherent trends of the freely run and the GCB2019 (Fig. 2A).

The initialized and uninitialized simulations show a comparably good match to GCB2019 with respect to net carbon flux into the ocean (with high correlation of 0.98), it suggests the good representation of the ocean carbon sink variations (especially on decadal timescale) in the historical free run. This implies that these variations of the globally integrated ocean carbon sink are more from external forcing rather than internal variability (McKinley et al., 2020).

The net carbon flux into the land shows higher correlation for initialized simulations at lead time of 2 years than that for uninitialized simulations. This indicates the interannual variations are better captured in the initialized model system even after 2 years of free integration. This result implies a predictability of the air-land CO_2 flux of at least 2 years.

We further quantify the predictive skill of the global carbon cycle (Fig. 3). The correlation skill relative to GCB2019 is significant for the lead time of 5 years in atmospheric carbon growth and the ocean carbon sink, however, the skill is lower up to 2 years for the air-land CO_2 flux (Fig. 3A-C). The improved predictive skill of initialized hindcasts comparing to the historical uninitialized run is at lead time of 1 year for atmospheric carbon growth and at lead time of 2 years for air-land CO_2 flux. The detrended results (Fig. 3D-F) are similar to those from the original time series. The correlation of atmospheric carbon growth at a lead time of 2 years in the initialized hindcasts are higher than the uninitialized historical run when detrended. This indicates the contribution of a linear trend to the skill of uninitialized historical runs.

From our MPI-ESM1.2-LR initialized hindcasts, we find that predictive skill of air-sea CO_2 flux is relatively high up to 5 years, that of the air-land CO_2 fluxes is up to 2 years. This is consistent with previous studies without interactive carbon cycle, i.e., (Ilyina et al., 2021; Lovenduski, Bonan, et al., 2019; Lovenduski, Yeager, et al., 2019). Here we extend the prediction system into emission-driven enabling prognostic CO_2 and the system keeps the features of predictability. Furthermore, the prognostic CO_2 from the novel emission-driven decadal prediction system suggests predictability as well, and the atmospheric CO_2 growth rate shows predictive skill of 2 years in the initialized predictions.

5 Atmospheric CO_2 concentration

Fig. 4 shows time series of atmospheric CO_2 concentration from MPI-ESM simulations together with the NOAA_GML observations for the last decade. As the atmospheric CO_2 concentration is an accumulative quantity and shows mainly a linear increasing trend, it is necessary to zoom in to visualize the trend slope changes. In addition, the deviation of model simulated atmospheric CO_2 relative to observations in the previous period is accumulated along with the integration of the model, therefore, it ends up with 8ppm higher global atmospheric CO_2 concentration in the model simulation than in the observations (see Fig. S4). In the meanwhile, the NOAA_GML data represents the average of atmospheric CO_2 over marine surface sites (Dlugokencky & Tans, 2020), they are slightly smaller than the values on land because of the anthropogenic CO_2 emissions are mainly on land. The time series shown in Fig. 4 are bias corrected by removing the difference of mean states and linear trends between observation and simulations according to Boer et al. (2016).

The shown atmospheric CO_2 concentration from assimilation follows quite well the evolution of NOAA_GML observation, however the uninitialized historical run show larger deviation from the observation with root mean square error (RMSE) of 0.72 ppm whereas the RMSE for assimilation is 0.22 ppm (Fig. 4A). The initialized simulations could represent the observed evolution well even at lead time of 5 years, with lower RMSE of 0.46 ppm than uninitialized historical run. This result further demonstrate the ability of ESM-based decadal prediction system in reconstructing and predicting the global carbon cycle, with only assimilating the physical atmosphere and ocean fields.

6 Conclusions

For the first time, we extend a decadal prediction system based on MPI-ESM to integrate the interactive carbon cycle, driven by fossil fuel emissions, and hence enabling prognostic atmospheric CO_2. This new setup of assimilation and initialized predictions opens one more dimension of freedom, i.e., enabling prognostic atmospheric CO_2 and the corresponding interactive effects, and represents the global carbon cycle closer to the real world.

The variations of atmospheric carbon growth rate and CO_2 fluxes among atmosphere, ocean, and land are well reconstructed in our assimilation simulations, with high correlations (0.75, 0.97, and 0.75) with the GCB2019. This enables an internally consistent quantification of the global carbon budget within an Earth system model. Furthermore, our reconstruction of the global carbon cycle provides an additional line of evidence for quantifying the annual global carbon budgets and opens new opportunities in assessing the efficiency of carbon sinks and internally consistent metrics. In particular, this approach eliminates the budget imbalance term that arises in GCBs due to the combination of various, not fully consistent model and data approaches.

We also make a step forward and present retrospective predictions of the global carbon cycle which show predictive skill up to 5 years for air-sea CO_2 fluxes and up to 2 years for air-land CO_2 fluxes and the atmospheric carbon growth rate. The variations of atmospheric CO_2 are better reproduced in the assimilation and retrospective predictions than in the uninitialized historical simulations with prognostic CO_2 while the trend is better reproduced in the uninitialized simulations.

We keep the high predictive power of the prediction system by turning it from concentration-driven to emission-driven, and that still captures atmospheric CO_2 increase pretty well. But the emission-driven decadal prediction system delivers the huge advantage of simulating the land and ocean fluxes in response to fossil-fuel and land use change emissions, including all feedbacks. Further efforts, towards increasing observations to initiate the ESMs and to assess the predictive skills and providing reliable global estimate and spatial distribution of anthropogenic and natural emissions, will lead to more reliable reconstruction and predictions.

We demonstrate that our emission-driven decadal prediction system shows capability to reconstruct and predict the global carbon cycle and atmospheric CO_2 concentration variations. This will be a powerful tool in supporting the global carbon stocktaking and policy to compliance with goals of the Paris Agreement. Further multi-model simulations will alleviate dependence of individual model responses and hence demonstrate robust changes of the global carbon cycle.

Acknowledgments

Funding: H.L. and T.I. were supported by the Federal Ministry of Education and Research in Germany (BMBF) through the research program MiKlip (grant no. 01LP1517B), the European Union's Horizon 2020 research and innovation program under grant agreement no. 641816 (CRESCENDO), the European Union's Horizon 2020 research and innovation program under grant agreement no. 821003 (4C). We thank Julia Nabel and Jochem Marotzke for internal reviewing this manuscript. We thank Veronika Gayler and Thomas Raddatz for providing script and forcing data for setting up MPI-ESM1.2-LR emission-driven simulations. We thank Yohei Takano for running 4 members of uninitialized simulations and Kameswar Modali for helping set up the assimilation and initialized simulations. Simulations were performed at the German Climate Computing Center (DKRZ). Author contributions: H.L. designed this study and wrote the paper together with T.I., T.L., and J.P.. H.L. ran the MPI-ESM simulations and performed the analyses. T.L. ran the CBALONE module simulations. All authors discussed the results and commented on the manuscript at every stage. Data and materials availability: Primary data and scripts used in the analysis that may be useful in reproducing the authors' work are archived by the Max Planck Institute for Meteorology and can be obtained via the institutional repository http://hdl.handle.net/21.11116/0000-0009-6B84-A.

References

Ballantyne, A. á., Alden, C. á., Miller, J. á., Tans, P. á., & White, J. (2012). Increase in observed net carbon dioxide uptake by land and oceans during the past 50 years. *Nature*, *488*(7409), 70–72.

Balmaseda, M. A., Mogensen, K., & Weaver, A. T. (2013). Evaluation of the ecmwf ocean reanalysis system oras4. *Quarterly journal of the royal meteorological society*, *139*(674), 1132–1161.

Bastos, A., O'Sullivan, M., Ciais, P., Makowski, D., Sitch, S., Friedlingstein, P., ... others (2020). Sources of uncertainty in regional and global terrestrial co2 exchange estimates. *Global Biogeochemical Cycles*, *34*(2), e2019GB006393.

Boer, G. J., Smith, D. M., Cassou, C., Doblas-Reyes, F., Danabasoglu, G., Kirtman, B., ... others (2016). The decadal climate prediction project (DCPP) contribution to CMIP6. *Geoscientific Model Development (Online)*, *9*(10).

Bunzel, F., Notz, D., Baehr, J., Müller, W. A., & Fröhlich, K. (2016). Seasonal climate forecasts significantly affected by observational uncertainty of arctic sea ice concentration. *Geophysical Research Letters*, *43*(2), 852–859.

Canadell, J. G., Le Quéré, C., Raupach, M. R., Field, C. B., Buitenhuis, E. T., Ciais, P., ... Marland, G. (2007). Contributions to accelerating atmospheric co2 growth from economic activity, carbon intensity, and efficiency of natural sinks. *Proceedings of the national academy of sciences*, *104*(47), 18866–18870.

Dee, D. P., Uppala, S. M., Simmons, A., Berrisford, P., Poli, P., Kobayashi, S., ... others (2011). The era-interim reanalysis: Configuration and performance of the data assimilation system. *Quarterly Journal of the royal meteorological society*, *137*(656), 553–597.

Dlugokencky, E., & Tans, P. (2020). Trends in atmospheric carbon dioxide. *National Oceanic and Atmospheric Administration, Global Monitoring Laboratory (NOAA_GML)*. Retrieved from `https://gml.noaa.gov/ccgg/trends/`

Fransner, F., Counillon, F., Bethke, I., Tjiputra, J., Samuelsen, A., Nummelin, A., & Olsen, A. (2020). Ocean biogeochemical predictionsâinitialization and limits of predictability. *Frontiers in Marine Science*, *7*, 386. Retrieved from `https://www.frontiersin.org/article/10.3389/fmars.2020.00386` doi: 10.3389/fmars.2020.00386

Friedlingstein, P., Jones, M. W., O'Sullivan, M., Andrew, R. M., Hauck, J., Peters, G. P., ... Zaehle, S. (2019). Global carbon budget 2019. *Earth System Science Data*, *11*(4), 1783–1838. Retrieved from `https://essd.copernicus.org/articles/11/1783/2019/` doi: 10.5194/essd-11-1783-2019

Friedlingstein, P., O'Sullivan, M., Jones, M. W., Andrew, R. M., Hauck, J., Olsen, A., … others (2020). Global carbon budget 2020. *Earth System Science Data*, *12*(4), 3269–3340.

Goddard, L., Kumar, A., Solomon, A., Smith, D., Boer, G., Gonzalez, P., … others (2013). A verification framework for interannual-to-decadal predictions experiments. *Climate Dynamics*, *40*(1-2), 245–272.

Ilyina, T., Li, H., Spring, A., Müller, W. A., Bopp, L., Chikamoto, M. O., … others (2021). Predictable variations of the carbon sinks and atmospheric co2 growth in a multi-model framework. *Geophysical Research Letters*, *48*(6), e2020GL090695.

Ilyina, T., Six, K. D., Segschneider, J., Maier-Reimer, E., Li, H., & Núñez-Riboni, I. (2013). Global ocean biogeochemistry model HAMOCC: Model architecture and performance as component of the MPI-Earth system model in different CMIP5 experimental realizations. *Journal of Advances in Modeling Earth Systems*, *5*(2), 287–315.

Landschützer, P., Ilyina, T., & Lovenduski, N. S. (2019). Detecting regional modes of variability in observation-based surface ocean pco_2. *Geophysical Research Letters*, *46*(5), 2670–2679.

Li, H., & Ilyina, T. (2018). Current and future decadal trends in the oceanic carbon uptake are dominated by internal variability. *Geophysical Research Letters*, *45*(2), 916–925.

Li, H., Ilyina, T., Müller, W. A., & Landschützer, P. (2019). Predicting the variable ocean carbon sink. *Science advances*, *5*(4), eaav6471.

Li, H., Ilyina, T., Müller, W. A., & Sienz, F. (2016). Decadal predictions of the north atlantic co_2 uptake. *Nature communications*, *7*(1), 1–7.

Loughran, T., Boysen, L., Bastos, A., Hartung, K., Havermann, F., Li, H., … Pongratz, J. (2021). Past and future climate variability uncertainties in the global carbon budget using the mpi grand ensemble. *Global Biogeochemical Cycles*.

Lovenduski, N. S., Bonan, G. B., Yeager, S. G., Lindsay, K., & Lombardozzi, D. L. (2019). High predictability of terrestrial carbon fluxes from an initialized decadal prediction system. *Environmental Research Letters*, *14*(12), 124074.

Lovenduski, N. S., Yeager, S. G., Lindsay, K., & Long, M. C. (2019). Predicting near-term variability in ocean carbon uptake. *Earth System Dynamics (On-*

line), *10*(1).

Marotzke, J., Müller, W. A., Vamborg, F. S., Becker, P., Cubasch, U., Feldmann, H., ... others (2016). MiKlip: A national research project on decadal climate prediction. *Bulletin of the American Meteorological Society*, *97*(12), 2379–2394.

Mauritsen, T., Bader, J., Becker, T., Behrens, J., Bittner, M., Brokopf, R., ... others (2019). Developments in the MPI-M Earth System Model version 1.2 (MPI-ESM1. 2) and its response to increasing co_2. *Journal of Advances in Modeling Earth Systems*, *11*(4), 998–1038.

McKinley, G. A., Fay, A. R., Eddebbar, Y. A., Gloege, L., & Lovenduski, N. S. (2020). External forcing explains recent decadal variability of the ocean carbon sink. *AGU Advances*, *1*(2), e2019AV000149.

Obermeier, W. A., Nabel, J. E., Loughran, T., Hartung, K., Bastos, A., Havermann, F., ... others (2021). Modelled land use and land cover change emissions–a spatio-temporal comparison of different approaches. *Earth System Dynamics*, *12*(2), 635–670.

Park, J.-Y., Stock, C. A., Yang, X., Dunne, J. P., Rosati, A., John, J., & Zhang, S. (2018). Modeling global ocean biogeochemistry with physical data assimilation: a pragmatic solution to the equatorial instability. *Journal of Advances in Modeling Earth Systems*, *10*(3), 891–906.

Paulsen, H., Ilyina, T., Six, K. D., & Stemmler, I. (2017). Incorporating a prognostic representation of marine nitrogen fixers into the global ocean biogeochemical model hamocc. *Journal of Advances in Modeling Earth Systems*, *9*(1), 438–464.

Peters, G. P., Le Quéré, C., Andrew, R. M., Canadell, J. G., Friedlingstein, P., Ilyina, T., ... others (2017). Towards real-time verification of CO2 emissions. *Nature Climate Change*, *7*(12), 848–850.

Pongratz, J., Reick, C. H., Houghton, R., & House, J. (2014). Terminology as a key uncertainty in net land use and land cover change carbon flux estimates. *Earth System Dynamics*, *5*(1), 177–195.

Reick, C. H., Gayler, V., Goll, D., Hagemann, S., Heidkamp, M., Nabel, J. E., ... Wilkenskjeld, S. (2021). Jsbach 3-the land component of the mpi earth system model: documentation of version 3.2.

Séférian, R., Berthet, S., & Chevallier, M. (2018). Assessing the decadal predictability of land and ocean carbon uptake. *Geophysical Research Letters*, *45*(5), 2455–2466.

Spring, A., Dunkl, I., Li, H., Brovkin, V., & Ilyina, T. (2021). Trivial improvements of predictive skill due to direct reconstruction of global carbon cycle. *Earth System Dynamics Discussions*, 1–36.

Spring, A., & Ilyina, T. (2020). Predictability horizons in the global carbon cycle inferred from a perfect-model framework. *Geophysical Research Letters*, *47*(9), e2019GL085311.

Spring, A., Ilyina, T., & Marotzke, J. (2020). Inherent uncertainty disguises attribution of reduced atmospheric co2 growth to co2 emission reductions for up to a decade. *Environmental Research Letters*, *15*(11), 114058.

Uppala, S. M., Kållberg, P., Simmons, A., Andrae, U., Bechtold, V. D. C., Fiorino, M., ... others (2005). The era-40 re-analysis. *Quarterly Journal of the Royal Meteorological Society: A journal of the atmospheric sciences, applied meteorology and physical oceanography*, *131*(612), 2961–3012.

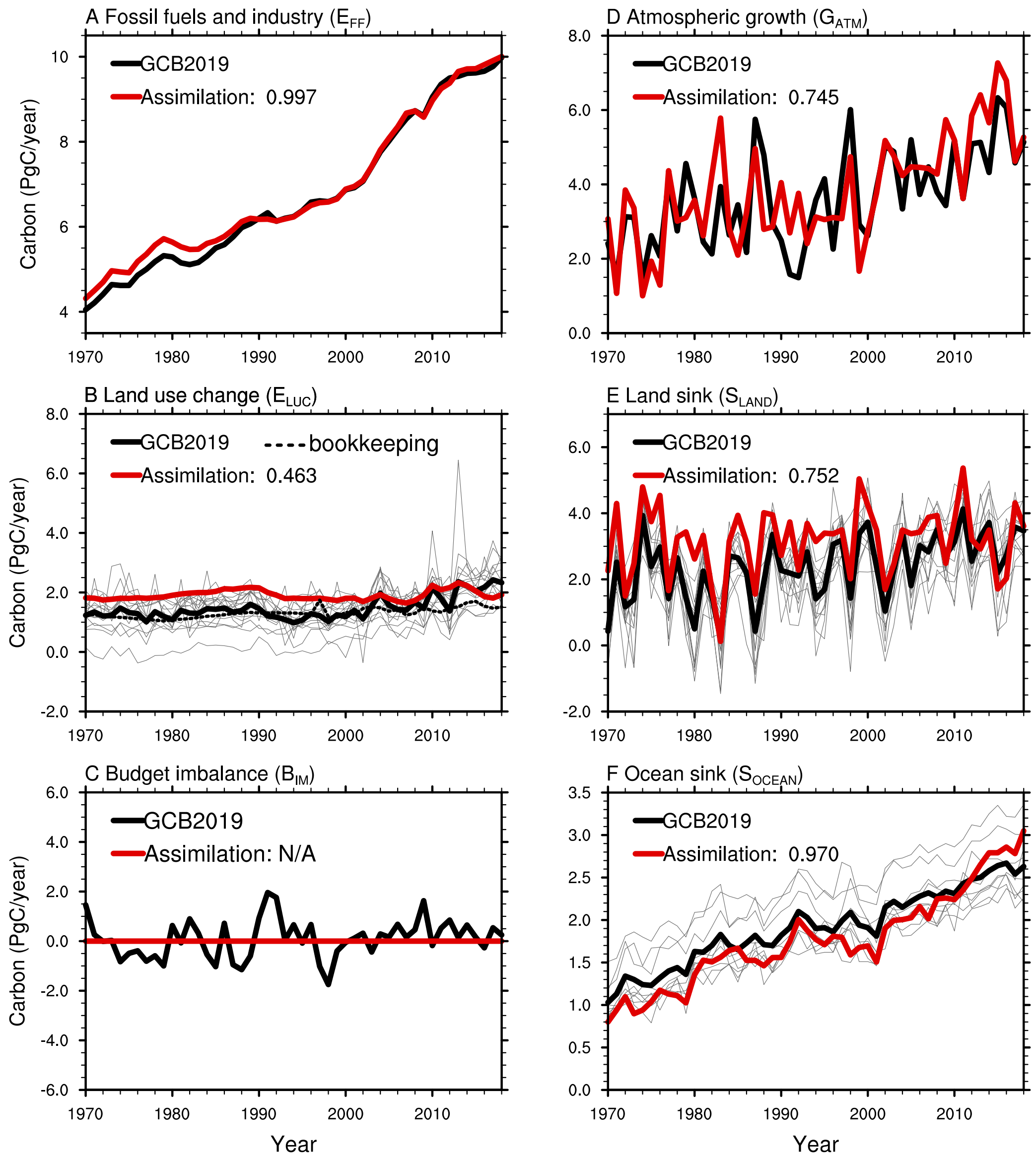

Figure 1. Time series of (A) fossil fuel and industry CO_2 emissions (E_{FF}), (B) emissions from land use change (E_{LUC}), (C) the budget imbalance (B_{IM}) that is not accounted for by the other terms, (D) atmospheric carbon growth rate (G_{ATM}), (E) the natural terrestrial carbon fluxes (S_{LAND}), and (F) air-sea CO_2 fluxes (S_{OCEAN}) from MPI-ESM1.2-LR assimilation in comparison with Global Carbon Budget (GCB 2019 (Friedlingstein et al., 2019)). Emissions (A & B) are positive when they are fluxes into the atmosphere, while sinks (D, E & F) are positive as fluxes into the respective compartment. A positive B_{IM} means a higher sum of emissions than sinks. The thin grey curves in B, E, and F show individual GCB stand-alone model results. The numbers in the legend show the correlation coefficients between assimilation and GCB2019.

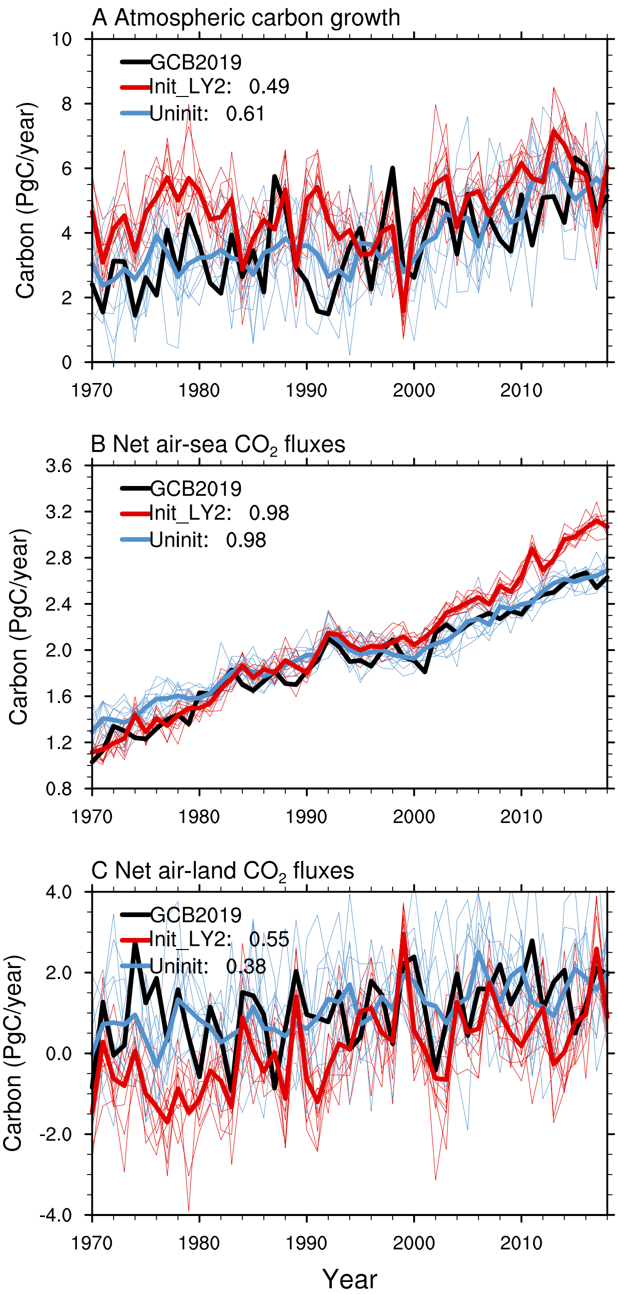

Figure 2. Time series of initialized simulations at lead time of 2 years in atmospheric carbon growth rate, i.e., G_{ATM} (A), net air-sea CO_2 fluxes, i.e., S_{OCEAN} (B) and net air-land CO_2 fluxes, i.e., E_{LUC}+S_{LAND} (C) together with Global Carbon Budget (GCB 2019 (Friedlingstein et al., 2019)). The shown time series are based on annual mean data for the time period from 1970-2018. Positive values in B-C refer to CO_2 fluxes into the ocean or land. The numbers in the legend show the correlation coefficients between the simulations and GCB2019, the ensemble mean data is used for the calculation.

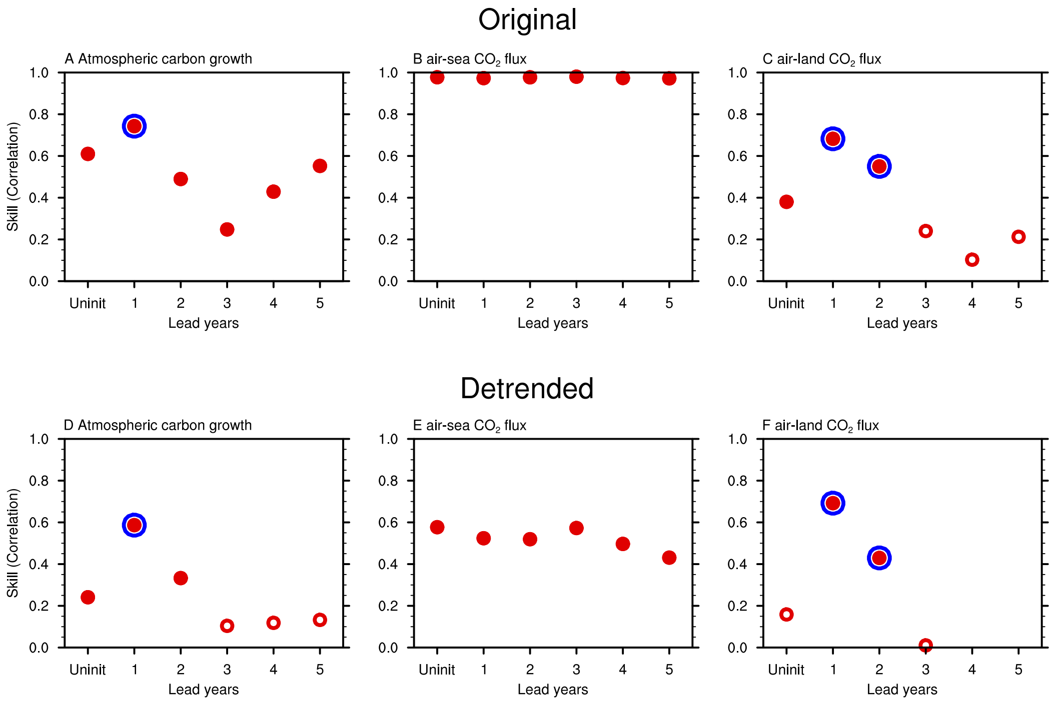

Figure 3. Predictive skill of atmospheric carbon growth rate, i.e., G_{ATM} (A and D), air-sea CO_2 fluxes, i.e., S_{OCEAN} (B and E) and net air-land CO_2 fluxes, i.e., E_{LUC}+S_{LAND} (C and F) reference to Global Carbon Budget (GCB 2019 (Friedlingstein et al., 2019)). A-C show results of anomaly correlation coefficients from the original time series, and D-F show results from the detrended time series with red open circles. All are based on annual mean time series for the time period from 1970-2018. The filled red circles on top of the open red circles show that the predictive skill is significant at 95% confidence level and the additional larger blue circles indicate improved significant predictive skill due to initialization in comparison to the uninitialized simulations. We use a nonparametric bootstrap approach (Goddard et al., 2013) to assess the significance of predictive skill.

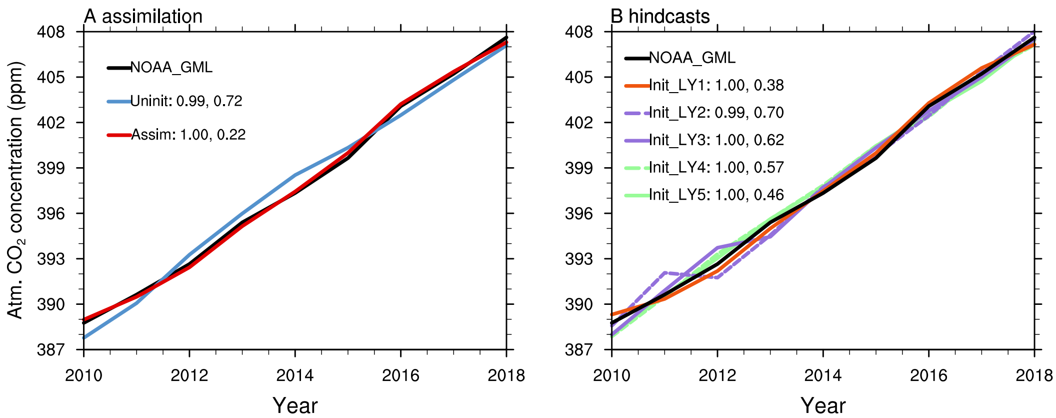

Figure 4. Atmospheric CO_2 concentration from the uninitialized (Uninit) and assimilation (Assim) simulations (A) and initialized simulations at lead time from 1-5 years (Init_LY1 to Init_LY5) (B) in comparing with observations in the last 10 years. The numbers in the figure legend show the correlation (left) and root mean square error (RMSE, right) of the simulations relative to observational data from NOAA_GML (Dlugokencky & Tans, 2020). The time series are bias corrected by removing the difference of mean states and linear trend between observation and simulations according to Boer et al. (2016).

Supporting Information for "Reconstruction and prediction of the global carbon cycle with an emission-driven Earth System Model"

H. Li[1], T. Ilyina[1], T. Loughran[2], J. Pongratz[1,2]

[1]Max Planck Institute for Meteorology, Hamburg, Germany

[2]Department of Geography, Ludwig Maximilian University, Munich, Germany

Contents of this file

1. Figures S1 to S4
2. Tables S1 to S1

References

Dlugokencky, E., & Tans, P. (2020). Trends in atmospheric carbon dioxide. *National Oceanic and Atmospheric Administration, Global Monitoring Laboratory (NOAA_GML)*. Retrieved from https://gml.noaa.gov/ccgg/trends/

Friedlingstein, P., Jones, M. W., O'Sullivan, M., Andrew, R. M., Hauck, J., Peters, G. P., ... Zaehle, S. (2019). Global carbon budget 2019. *Earth System Science Data*, *11*(4), 1783–1838. Retrieved from https://essd.copernicus.org/articles/11/1783/2019/ doi: 10.5194/essd-11-1783-2019

Marotzke, J., Müller, W. A., Vamborg, F. S., Becker, P., Cubasch, U., Feldmann, H., ... others (2016). MiKlip: A national research project on decadal climate prediction. *Bulletin of the American Meteorological Society*, *97*(12), 2379–2394.

Table S1. Simulations based on MPI-ESM1.2-LR. Resolution Atmosphere: T63L47 Ocean: GR15L40. The design of the prediction simulations is according to previous study (Marotzke et al., 2016). The assimilation starts from the end of year 1958 in an uninitialized simulation. The nudging is strong therefore an assimilation starting from a different uninitialized simulation would end up with similar evolution of the climate and carbon cycle. The initialized simulations start from the assimilation yearly from October 31st and run freely for 2 months plus 5 years afterwards. We have 59 runs for one ensemble of initialized simulations starting from 1960 to 2019 annually and run for 5 years and 2 months each, i.e., Nov. 1960 - Dec. 1965 for starting year 1960, Nov. 1961 - Dec. 1966 for starting year 1961, and so forth until Nov. 2018 - Dec. 2023. The ensembles are generated with lagged 1-day initialization, i.e., the simulations start from 10 consecutive days from October 31st to November 9th. The ensembles for uninitialized simulations are generated by starting from different year of the control simulation.

Simulations	Ensemble members	Nudging	Initial condition	Time period
Uninitialized	10	N/A	Preindustrial	1850-2099
Assimilation	1	Atm.: ERA Ocean: ORAS4 anomalies (without 5N-5S band) Sea Ice: NSIDC	Uninitialized	1959-2018
Initialized	10	N/A	Assimilation	1960-1965 ... 2018-2023

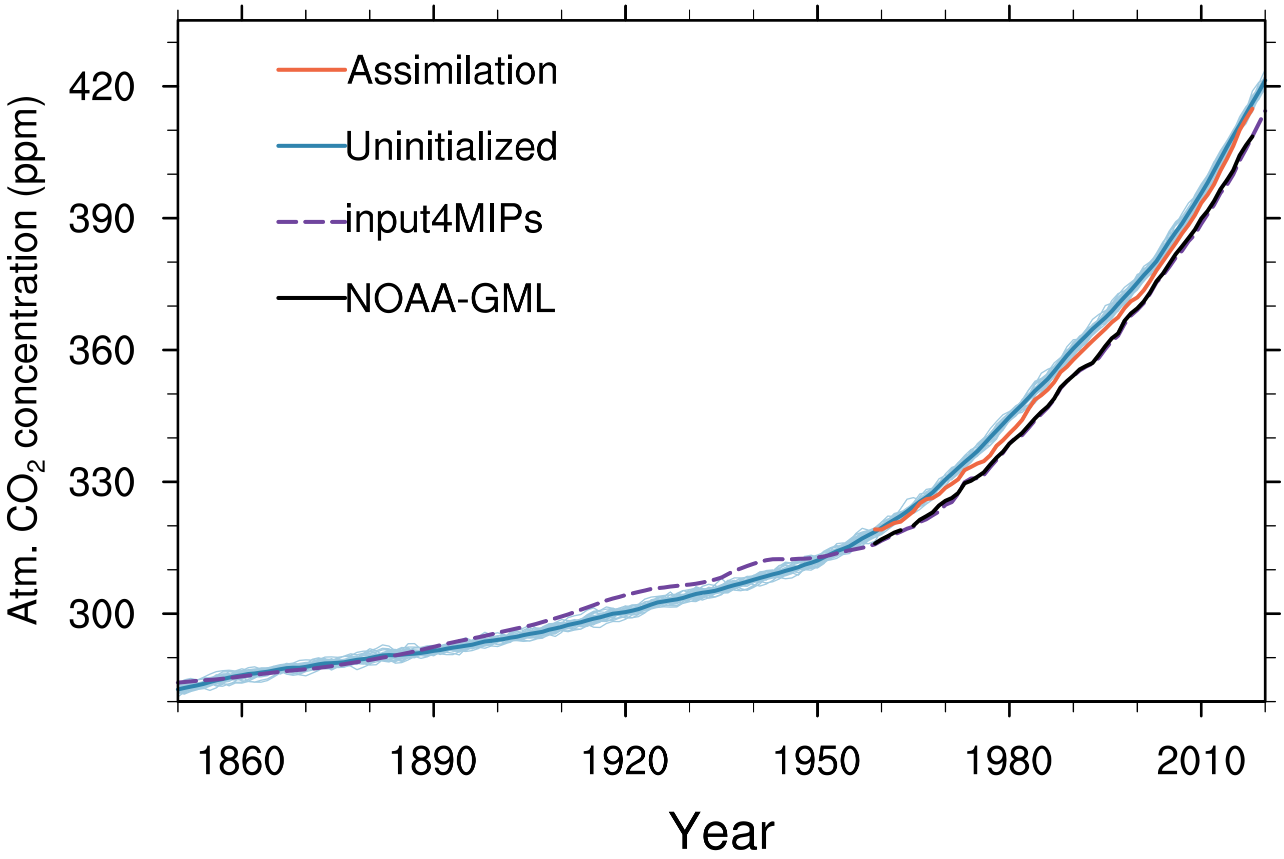

Figure S1. Time series of atmospheric CO_2 concentration from model simulations and observation from 1850-2020. The assimilation and uninitialized simulations are shown with orange and blue solid lines, respectively. The CMIP6 input4MIPs atmospheric CO_2 concentration forcing and the NOAA_GML observation (Dlugokencky & Tans, 2020) are shown with blue dashed line and black solid lines, respectively.

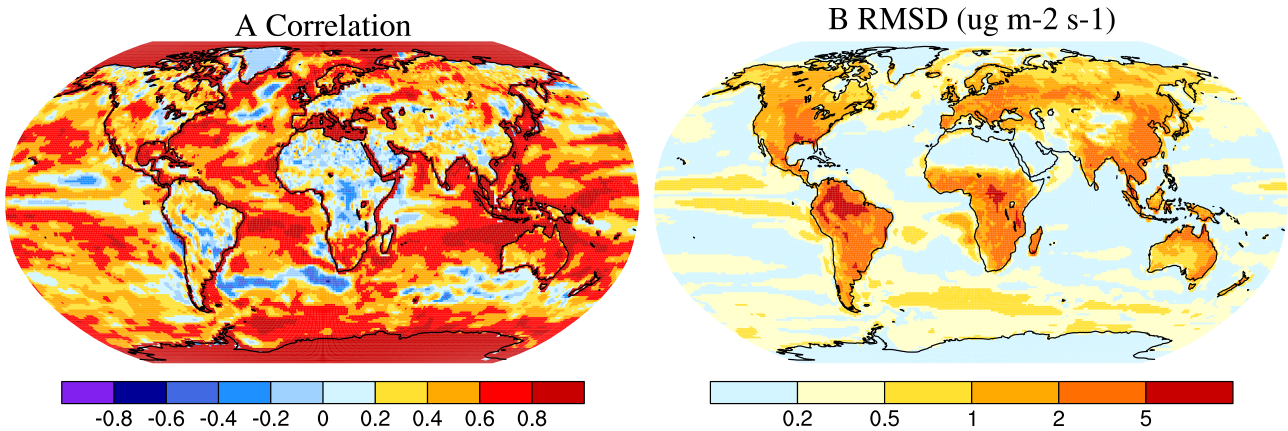

Figure S2. Spatial distribution of correlation and root mean square difference (RMSD) in air-sea and air-land CO_2 fluxes between Global Carbon Budget (GCB 2019 (Friedlingstein et al., 2019)) multi-model mean and MPI-ESM1.2-LR assimilation. The statistics are based on annual mean time series for the time period from 1960-2018.

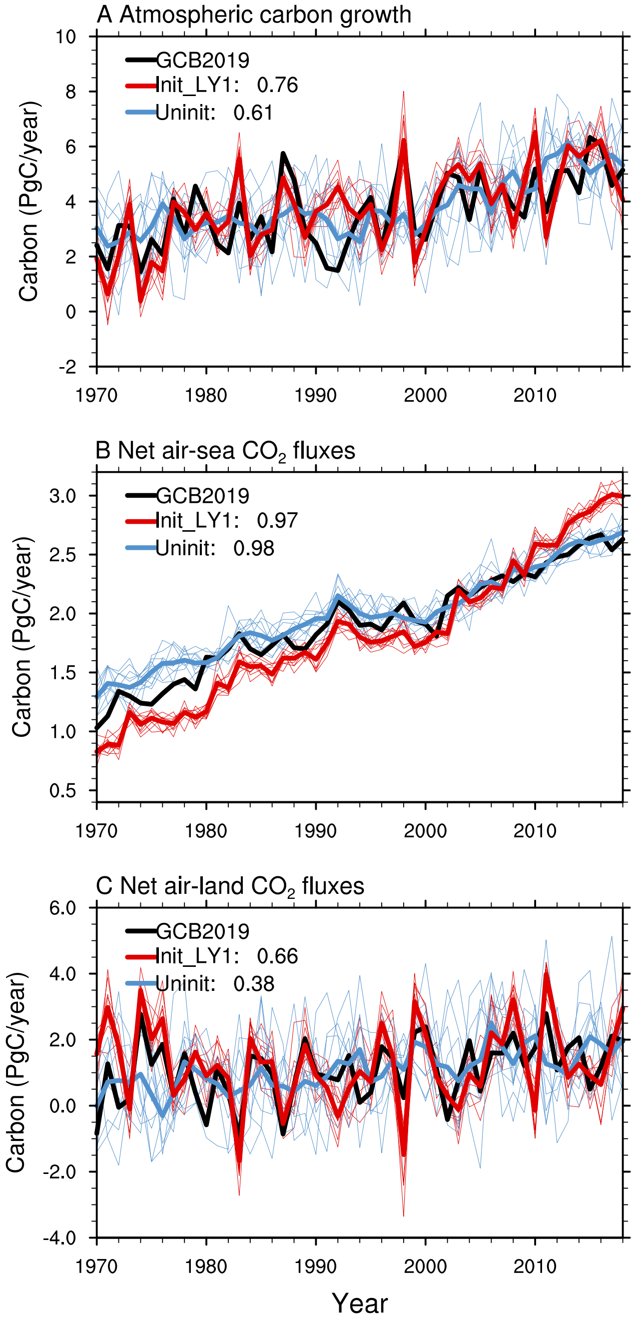

Figure S3. Time series of initialized simulations at lead time of 1 year in atmospheric carbon growth rate, i.e., G_{ATM} (A), net air-sea CO_2 fluxes, i.e., S_{OCEAN} (B) and net air-land CO_2 fluxes, i.e., E_{LUC}+S_{LAND} (C) together with Global Carbon Budget (GCB 2019 (Friedlingstein et al., 2019)). The shown time series are based on annual mean data for the time period from 1970-2018. Positive values in B-C refer to CO_2 fluxes into the ocean or land. The numbers in the legend show the correlation coefficients between the simulations and GCB2019, the ensemble mean data is used for the calculation.

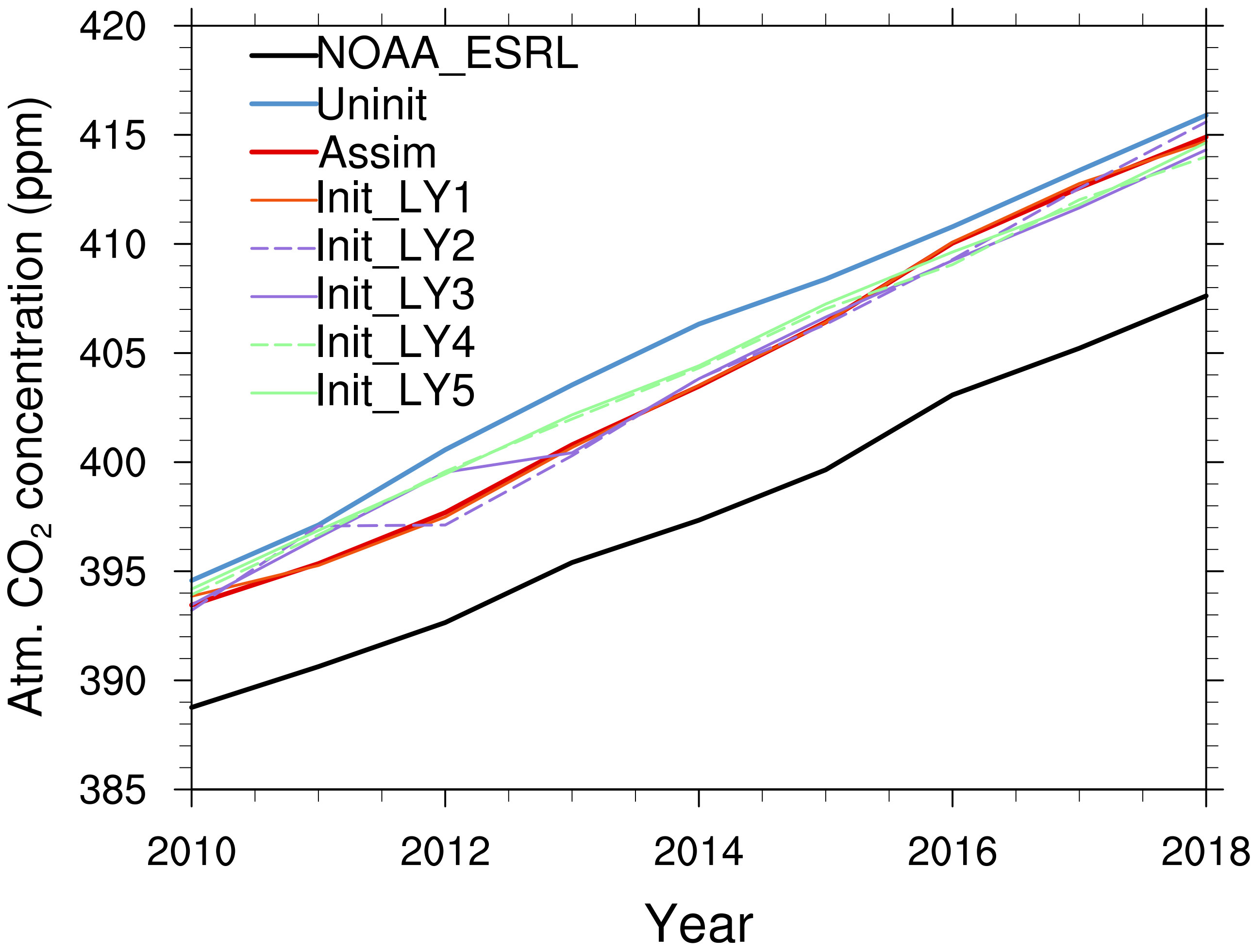

Figure S4. Atmospheric CO_2 concentration from the assimilation and initialized simulations together with NOAA_GML observation (Dlugokencky & Tans, 2020) in the last 10 years. The time series are original model outputs and connected according to the lead time of years.